Optics and Lasers in Engineering **4** (1983) 25–38

Surface Stress Meters Utilising the Optical Waveguide Effect of Chemically Tempered Glasses

Toru Kishii

R and D Center, Toshiba Corp., Kawasaki 210; and Toshiba Glass Co., Yoshida, 421-03 Japan

(Received: 11 March 1982)

ABSTRACT

Chemical tempering is increasing the areas of glass application in the wristwatch, glass and electronic industries. The optical waveguide effect in the surface layer of chemically tempered glass is a useful tool for measuring surface stress for quality and process control purposes. The theoretical basis, measuring techniques and apparatus are briefly reviewed.

1. INTRODUCTION

Chemical tempering is industrially applied for the following glasswares:

Wristwatch crystals
Eyeglass lenses
Protective goggles for welders
Glass bottles and cups
Curved mirrors
Automobile mirrors
Jet aircraft windshields
Photomask glass
High power glass laser rods
Bulb glass for high power electron tubes.

Optics and Lasers in Engineering 0143-8166/83/0004-0025/$03·00—

Ion-exchange (Na^+ in glass) $\leftrightarrow$ (K^+ in KNO_3 melt) at a glass surface forms a compression layer.[1] The layer reinforces glass-ware mechanical strength by almost one order of magnitude.

The surface compression in chemically tempered glass correlates with the mechanical strength of the glass and the compression layer thickness correlates with the resistance against strength reduction by scratching and weathering. Therefore, surface compression and compression layer thickness are important for quality and process control of tempered glass-wares.

2. OPTICAL EFFECT IN A CHEMICALLY TEMPERED GLASS SURFACE

Ion-exchange also forms a refractive index gradient in the surface layer. This layer causes peculiar optical effects. Several interpretations of the effects and the methods for evaluating surface stress based on these effects have been proposed.[2–4]

On the other hand, optical waveguide effects in graded refractive index (GRIN) layers of chemically tempered glasses have been found and analysed in fibre optics and optical integration technologies. Ion-exchange has been a highly effective tool for forming many kinds of opto-electronic and integrated optical devices, such as light modulators, light deflectors, Selfoc® optical fibres and lenses. Photoelastic birefringences in the layers have been experimentally detected,[5] and finally Jausaund and Chartier have suggested the possibility of surface stress measurement using the effect.[6]

Optical waveguide theory, in combination with a ray optical model, gave a simple procedure for surface stress measurement of chemically tempered glass[7] (cf. Sections 3–5). Moreover, the theory forecast the possibility of:

(i) Surface stress measurement of chemically tempered curved glass surfaces;[8]
(ii) Surface stress measurement of thermally tempered float glasses by using the optical waveguide effect in tin-diffused surface layers;[9]
(iii) Surface stress measurement of thermally tempered glasses by using the optical waveguide effect of surface striation layers;[10]

(iv) Surface stress measurement of tempered glasses by using optical surface waves, such as a critical ray.[11,12]

3. PRINCIPLE

When optically excited, a GRIN layer sustains guided waves. Optical waves propagate in the layer as discrete modes or modes of finite number. Each mode has its own effective refractive index n_{eff}, which is represented by

$$n_{\text{eff}} = \frac{\text{Light velocity in vacuum } c}{\text{Mode propagation velocity}}$$

The n_{eff} values of sustained modes depend on refractive index distribution $n(x)$ (n = refractive index, x = depth from the surface) in the layer.

The photoelastic effect in the GRIN layer causes a difference in refractive index between two linearly polarised component waves, which vibrate in directions perpendicular to (TM wave) and parallel with (TE wave) the surface, respectively (Fig. 1).

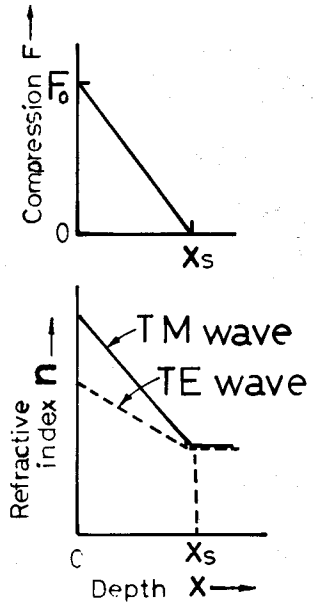

Fig. 1. Representation of stress and refractive index distributions with depth in the surface layer of chemically tempered glass.

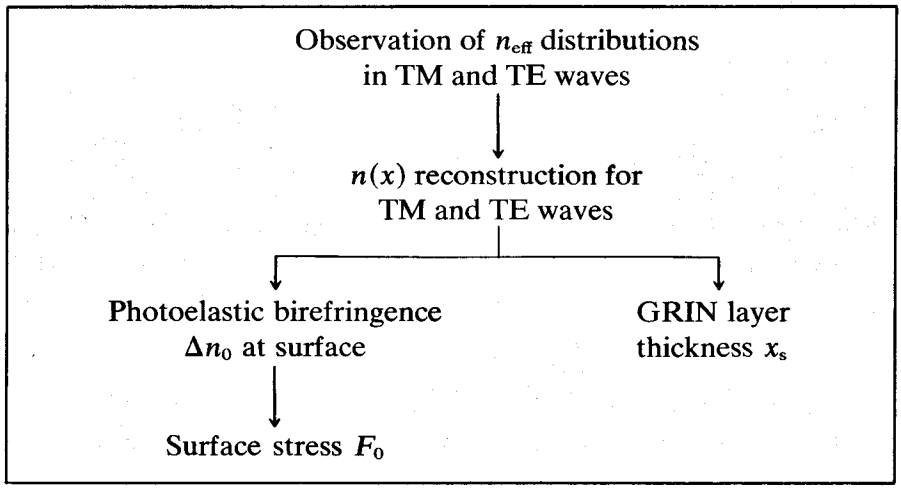

Fig. 2. Sequence for estimating F_0 and x_s.

Therefore, surface stress and compression layer thickness can be estimated by the sequence shown in Fig. 2.

4. MATHEMATICAL PROCEDURE

(a) Wave optical model

Propagation modes in a GRIN layer are represented by:[13]

$$A(x)\exp\{i(\omega t-\beta z)\} \tag{1}$$

with

$$\beta = 2\pi/\lambda$$

where x = depth from surface, t = time, z = distance along propagation path, $A(x)$ = amplitude distribution function, λ = light wavelength in the guide, and ω = angular velocity of vibration.

The quantity β and the function $A(x)$ can exist only when β satisfies the following condition:

$$\int_0^{x_b}\sqrt{n^2(x)k^2-\beta^2}\,dx = (N+\tfrac{3}{4})\pi \tag{2}$$

where $k = 2\pi/\lambda_0$, $n(x = x_b) = \beta/k$, N = an integer, $n(x)$ = distribution function for refractive index n, and λ_0 = light wavelength in vacuum.

In addition, the following relation is evident:

$$n_{\text{eff}} = \beta/k \equiv n(x = x_b) \tag{3}$$

(b) Ray optical model

Equations (1) and (2) are mathematically too complex to be solved for industrial quality control purposes. The formula, however, is simplified by referring to a ray optical model (Fig. 3).

Assume that a light flux with wavefront AA_1B_1B is introduced into a GRIN layer by incidence from an optically denser medium. Each ray, for example, A_1G_1, in the flux propagates in the layer along the ray optical path $\overrightarrow{G_1F_1G_2F_2, \ldots}$, with repeated reflections at $G_2, \ldots, .$

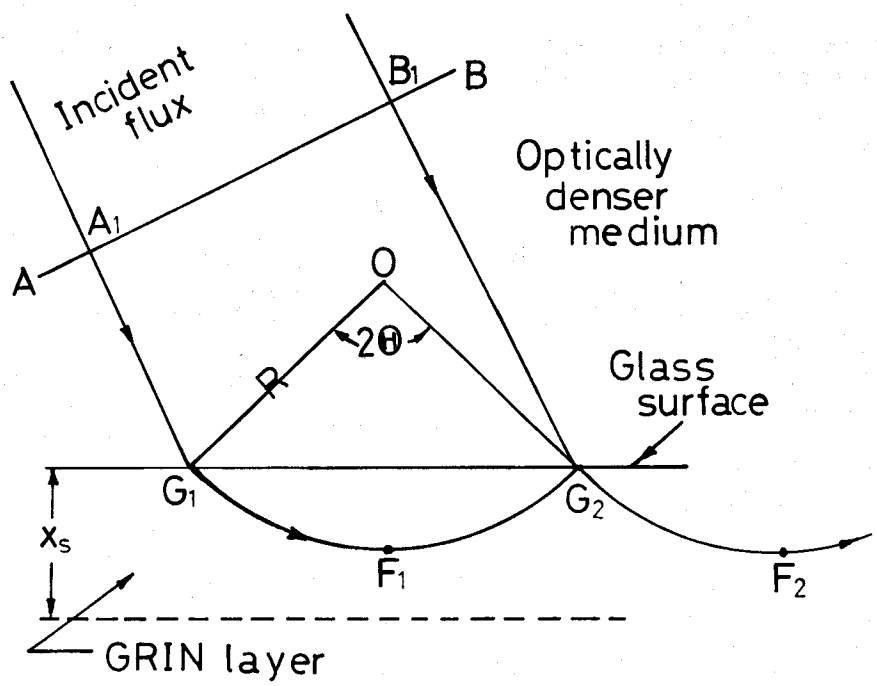

Fig. 3. Ray optical model of optical waveguide effect in a graded refractive index (GRIN) layer. AA_1B_1B = incident light flux wave front, $\overrightarrow{G_1F_1G_2}$ = mirage path, x_s = GRIN layer depth, O = centre of curvature for circular mirage path in the case of a linear GRIN layer, R = radius of curvature for the mirage path, and $F_1, \ldots,$ = turning points in mirage paths.

Equation (2) is equivalent to the expression:

(Optical path difference per one cycle of mirage path)
$\equiv$(optical path length along the path $\overrightarrow{A_1G_1F_1G_2}$)
$-$(optical path length along B_1G_2) $=(N+\frac{3}{4})\lambda_0$

In addition, n_{eff} is equal to the refractive index of glass at turning point F_1 in the ray optical path $\overrightarrow{G_1F_1G_2}$, and at F_1, $x = x_b$.

(c) Linear GRIN structure

For a simplified linear GRIN layer with

$$n(x) = n_0 - \alpha x, \qquad 0 \leq x \leq x_s$$
$$n(x) = n_s \equiv n_0 - \alpha x_s, \qquad x_s \leq x$$

(where $n_0 = n$ at surface ($x = 0$), $n_s = n$ at substrate ($x \geq x_s$), x_s = depth of the GRIN layer, and $\alpha \equiv (n_0 - n_s)/x_s$ = refractive index gradient), the mirage path can be approximated by a circular arc with radius of curvature

$$R \doteqdot n_0/\alpha$$

and eqn (2) is transformed into

$$\tfrac{2}{3} n_0 R\theta^3 \doteqdot \lambda(N+\tfrac{3}{4}) \tag{4}$$

where θ = half angle of $\widehat{G_1OG_2}$ (O = centre of mirage path curvature), and in addition,

$$n_{\text{eff}} = n_0 \cos\theta \doteqdot n_0\left(1 - \frac{\theta^2}{2}\right)$$

Although the conditions

$$\int_0^{x_b} \sqrt{n^2 k - \beta^2}\, dx = 0$$

or in other words,

$$x_b = 0, \qquad \theta = 0$$

do not correspond to a real propagation mode, it corresponds to a fictive mode with $n_{\text{eff}} = n_0$, which propagates along the surface.

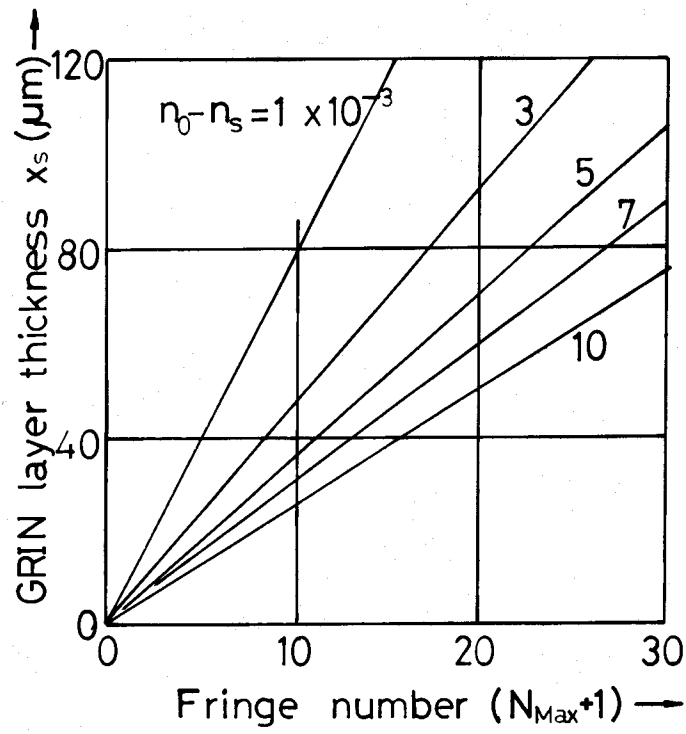

Fig. 4. Number of fringes ($N_{max}+1$) versus GRIN layer thickness x_s relations, with (n_0-n_s) as a parameter.

Equation (4) and experimental observation of n_{eff} for real modes in a GRIN layer allow n_0 determination by extrapolation.

Surface stress F_0 is given by:[3]

$$F_0 = \frac{\Delta n_0}{C} \equiv \frac{(n_0 \text{ for TM wave}) - (n_0 \text{ for TE wave})}{C}$$

where C = photoelastic constant of glass at the surface.

The condition

$$n_0 > n_{eff} \geq n_s$$

gives the number of TM or TE modes ($N_{max}+1$) as a function of x_s and (n_0-n_s), as shown in Fig. 4.

(d) Effect of n distribution

Excessive time and excessively high ion-exchange temperature often cause stress relaxation near the surface (Fig. 5). Maxima in stress and

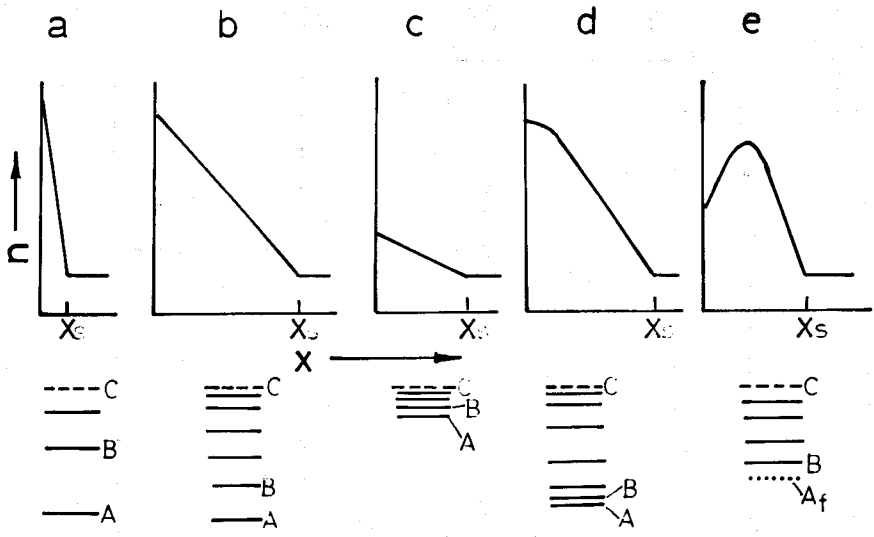

Fig. 5. Fringe pattern representations for various refractive index distributions. A = fringe with highest n_{eff}, C = position which corresponds to substrate refractive index n_s, A_f = faint fringe with highest n_{eff}.

refractive index distributions lie beneath the surface. This is identified in fringe patterns in which the highest effective refractive index fringes are faint (A_f in Fig. 5(e)).

The faint fringes correspond to propagation modes, which are trapped around the index maxima, as in the cases of GRIN or Selfoc® optical fibres. Birefringence, given by faint fringes, gives an approximate surface stress, not the maximum stress. Compression layer thickness is not given by such fringe patterns.

(e) Compatibility of models

It should be noted that the ray optical model is not always suitable for analysing propagation modes. For example, obtaining the mode propagation velocity by using the mirage path model is more complex and more inaccurate, compared to using C/n_{eff}. Moreover, the ray optical model gives false information on $A(x)$.

The compatibility between wave optical and ray optical models must be examined at each analysis.

5. EXPERIMENTAL OBSERVATION

(a) Flat surface

For n_{eff} distribution observation, two methods are applicable; namely,

Bright field (and dark fringe) method,
Dark field (and bright fringe) method (Fig. 6).

The latter detects propagation mode waves while the former detects refracted waves which lack propagation mode waves (Fig. 7). The dark field method is popular in integrated optics technology for n_{eff} analysis.

The fringe patterns allow determination of $n_0 - n_s$, Δn_0 and $(N_{max}+1)$ (Fig. 8).

An example of apparatus sensitivity is:

$$1 \text{ mm distance on telescope reticle} \rightarrow 28 \text{ kg mm}^{-2}$$

(b) Convex surface

The procedure is similar to that for a flat surface, except that fringes do not stand at infinity, but at finite distance[8] from the surface. Therefore, stress measurement sensitivity is modified, depending on radius of curvature for the surface.

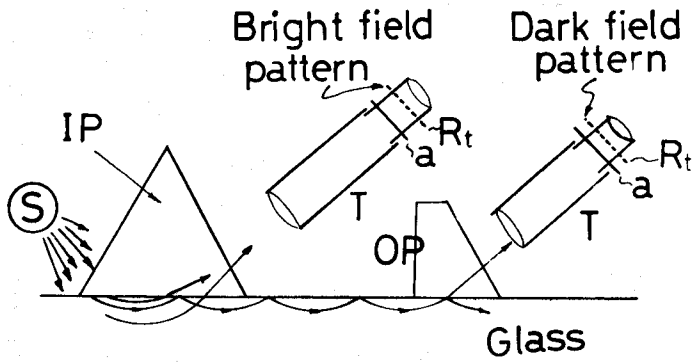

Fig. 6. Experimental setup for bright field and dark field pattern observations. S = monochromatic light source, IP = high index input prism, OP = high index output prism, T = telescope, R_t = reticle of telescope ocular lens, and a = analyser.

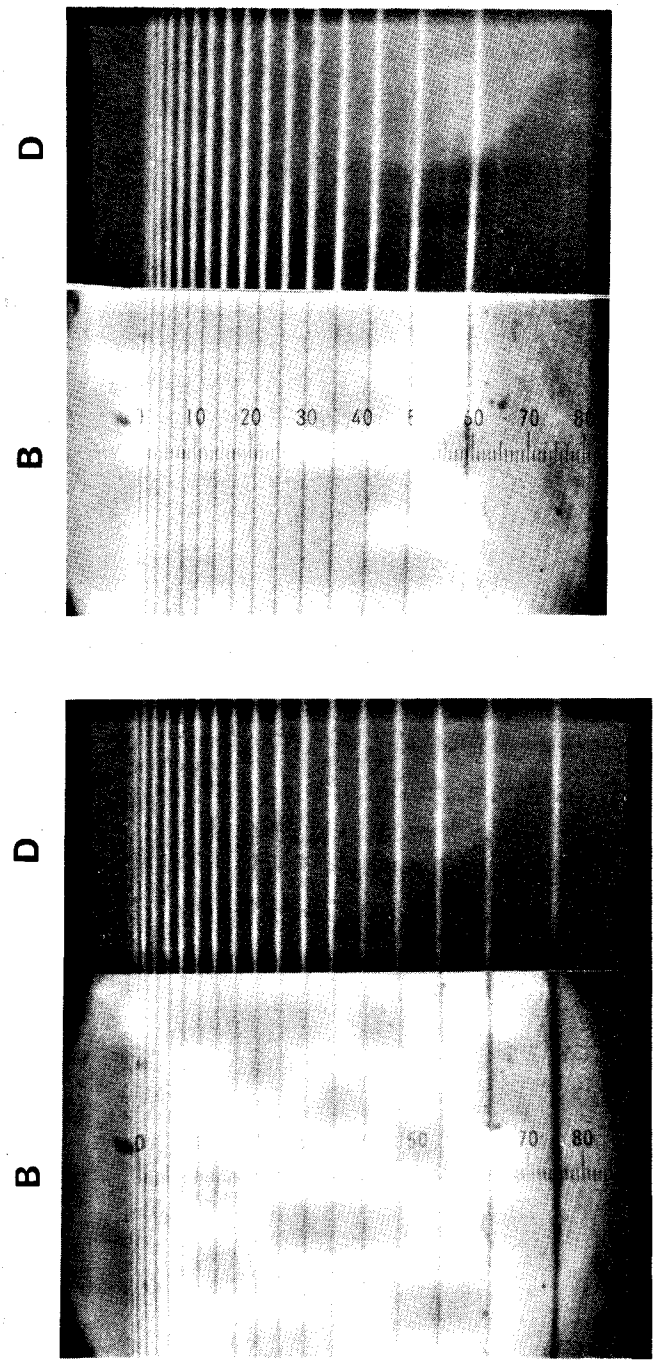

Fig. 7. Field patterns for a chemically tempered glass observed by TM (left) and TE (right) waves. Bright (B) and Dark (D) field patterns.

6. APPARATUS

For small-size flat tempered glass sheets, an FSM-10 surface stress meter is used (Fig. 9). It gives a bright view field and therefore measurement is very easy.

The FSM-30 surface stress meter is constructed so that the meter can be placed on medium- and large-size sample glass sheets (Fig. 10). It can be used for both flat and curved surfaces. Moreover, it can be used for thermally tempered float glasses.[9]

The FSM-40 surface stress meter is constructed to measure small-size curved and flat glass sheets (Fig. 11). It has rotatable separated prisms and gives a dark field.

Glasses for the electronics industry, such as photomask glasses, substrate glasses for optical audio-, video- and memory discs, and glasses for display devices, cannot have even microscopic scratches. FSM-60 is constructed for these glasses (Fig. 12).

Video display is possible for all the surface meters by placing a photo-electric target surface for an image tube just after the reticle (Fig. 9).

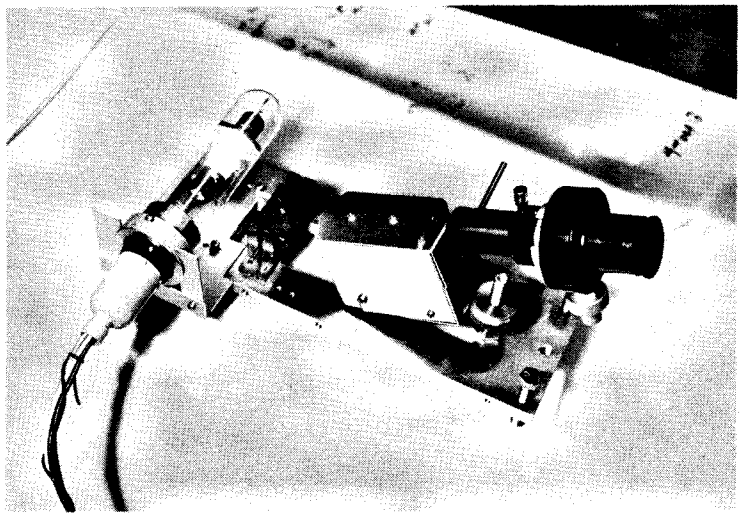

Fig. 10. FSM-30 surface stress meter for large-size flat and curved chemically tempered glass sheets.

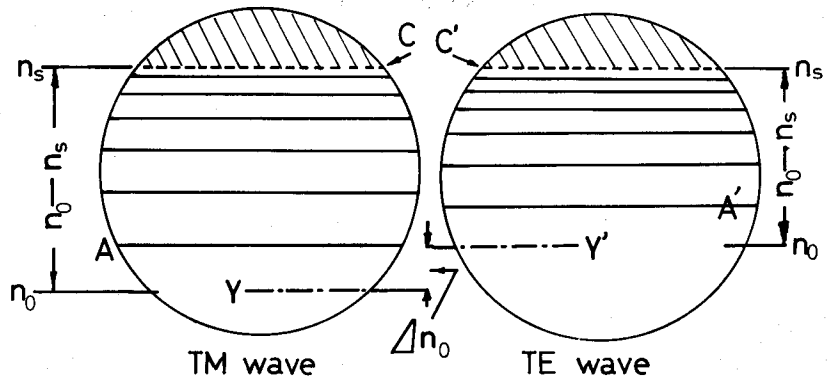

Fig. 8. Relation between fringe patterns and refractive index distributions. A and A′ = fringes with highest n_{eff} values in the patterns; C and C′ = boundaries between bright and dark areas which correspond to n_s; and Y and Y′ = fictive fringe positions with $n_{eff} = n_0$, obtained by extrapolation.

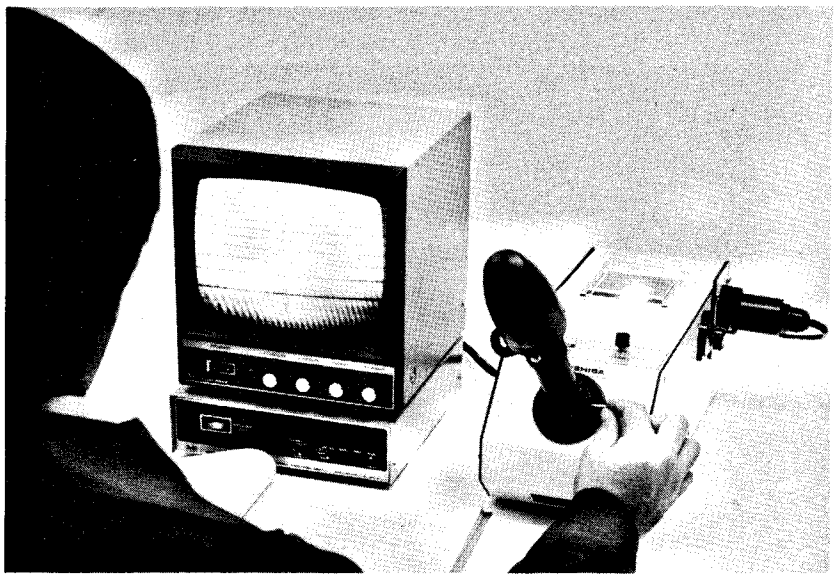

Fig. 9. FSM-10, surface stress meters, for small-size flat chemically tempered glass sheets (right), and equipped with a video display system (left).

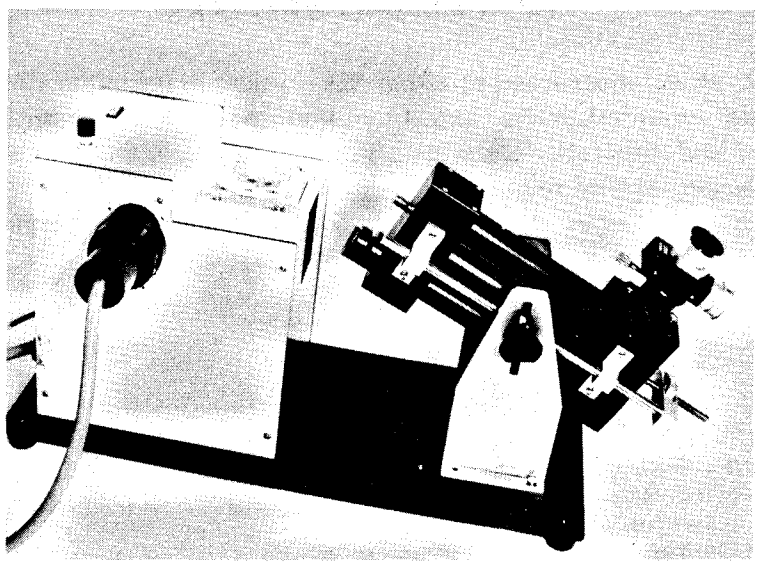

Fig. 11. FSM-40 surface stress meter for small-size flat and curved chemically tempered glass sheets.

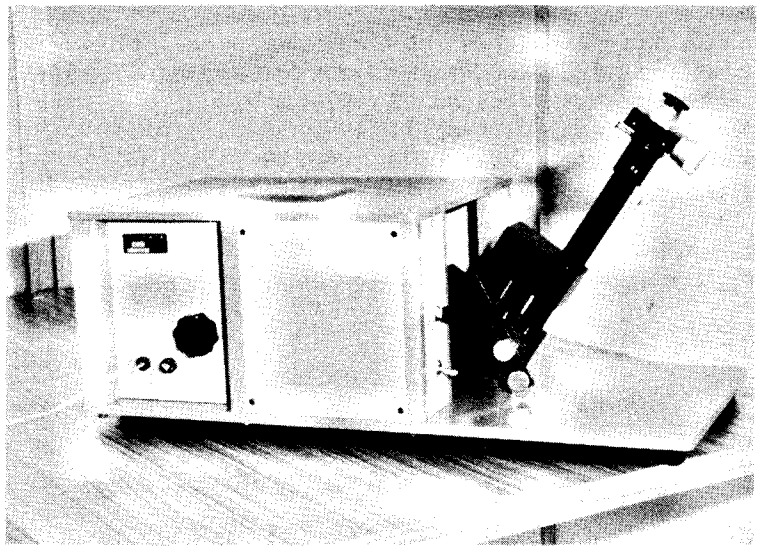

Fig. 12. FSM-60 surface stress meter for chemically tempered glasses for the electronics industry.

7. CONCLUDING REMARKS

Surface stress measurement using the optical waveguide effect is versatile, non-destructive and time and man-power saving. The method and apparatus are widely used in the Japanese wristwatch, eyeglass and optical industries.

The author hopes the apparatus described will help to improve productivity in these industries.

REFERENCES

1. M. E. Nordberg, E. L. Mochel, H. M. Garfinkel and J. S. Olcott, *J. Am. Ceram. Soc.*, **47** (1964) 215.
2. M. Hara, *Research Report of Asahi Glass Co.*, No. 21, 1971, p. 19.
3. B. Gänswein, *Glastech. Ber.*, **53** (1980) 220.
4. C. Guillemet, Thesis, L'Université de Paris, 27 May, 1968; *Proc. IUTAM Symp. on Optical Methods in Mechanics of Solid, Univ. Poitiers, France, 10–14 Sept., 1979*, Sijthoff & Noordhoff, Amsterdam, 1981.
5. T. G. Giallorenzi, E. J. West, R. Kirk, R. Ginther and R. A. Andrews, *Appl. Opt.*, **12** (1973) 1240.
6. P. C. Jaussaud and G. H. Chartier, *J. Phys. D. Appl. Phys.*, **10** (1977) 645.
7. T. Kishii, *Yōgyō-Kyokai-Shi* (*J. Ceram. Soc. Japan*), **87** (1979) 119.
8. T. Kishii, *Yōgyō-Kyokai-Shi* (*J. Ceram. Soc. Japan*), **86** (1978) 336.
9. T. Kishii, *Opt. Laser Technol.*, **11** (1979) 259.
10. T. Kishii, *Opt. Laser Technol.*, **11** (1979) 197.
11. T. Kishii, *Opt. Laser Technol.*, **12** (1980) 99.
12. T. Kishii, *Opt. Laser Technol.*, **13** (1981) 261.
13. D. Marcuse, *IEEE J. Quantum Electronics*, **QE-9** (1975) 1000.